Proceedings of the 1998 IEEE/RSJ
Intl. Conference on Intelligent Robots and Systems
Victoria, B.C., Canada • October 1998

Undetected Locked-Joint Failures in Kinematically Redundant Manipulators: A Workspace Analysis

M. Goel, A. A. Maciejewski, and V. Balakrishnan

Purdue University
School of Electrical and Computer Engineering
1285 Electrical Engineering Building
West Lafayette, Indiana 47907-1285

Abstract

Robots are frequently used for operations in hostile environments. The very nature of these environments, however, increases the likelihood of robot failures. Common failure tolerance techniques rely on effective failure detection. Since a failure may not always be successfully detected, or even if detected, may not be detected soon enough, it becomes important to consider the behavior of manipulators with undetected failures. This work focuses on developing techniques to analyze a manipulator's workspace and identify regions in which tasks, characterized by sequences of point-to-point moves, can be completed even with such failures. Measures of fault tolerance are formulated to allow for the evaluation of the workspace.

I. Introduction

Failures in robots occur frequently in industrial operations [1]. The likelihood of failures is far greater when robots are operated in harsh environments [2]. Since the control of the individual joints is essentially independent in a typical robotic system, most failures affect only a single joint. A common type of joint failure is the "locked joint", where the affected joint's velocity is identically zero. Such a failure may have catastrophic consequences, or, at the very least, significantly degrade the system performance.

Since immediate human attention for repair or recovery is often not practical in hostile environments, it is desirable that the robot itself be able to cope with failures. A common approach to enhancing failure tolerance capability in a robot is the incorporation of redundancy in the design. This may be in the form of duplicated components [3], or, through the intelligent utilization of kinematic redundancy [4, 5, 6, 7]. Though there has been considerable work in the area of failure tolerant systems, there remain significant questions about the post-fault behavior of robotic systems that do not incorporate fail-safe mechanisms. Existing failure tolerance schemes rely on effective failure detection; only after a failure is detected, is an appropriate failure recovery strategy initiated [8, 9]. Since failure detection is itself a difficult process that may not always be successful [10], it is important to address the problems associated with undetected failures.

In this work, the analysis of the post-fault behavior of manipulators with undetected locked-joint failures, presented in [11], is extended to establish a procedure for workspace analysis. This analysis allows for the identification of workspace regions for which task completion may be possible even with undetected failures. A general class of tasks characterized by sequences of point-to-point moves in task space is considered.

II. Mathematical Framework

The position and/or orientation (henceforth referred to as "position") of the end effector of a manipulator can be expressed in terms of its joint variables by the kinematic equation

$$\mathbf{x} = f(\mathbf{q}), \tag{1}$$

where $\mathbf{x} \in \mathbb{R}^m$ is the position of the end effector, $\mathbf{q} \in \mathbb{R}^n$ is the vector of joint variables, and m and n the dimensions of the task space and joint space respectively. Manipulators that have more degrees of freedom (DOFs) than required for a task, i.e., $n > m$, are said to be redundant. The end-effector velocity is expressed in terms of the joint rates as

$$\dot{\mathbf{x}} = J\dot{\mathbf{q}}, \tag{2}$$

where $J \in \mathbb{R}^{m \times n}$ is the manipulator Jacobian, $\dot{\mathbf{x}}$ is the end-effector velocity, and $\dot{\mathbf{q}}$ is the joint velocity.

If perfect servo control of the joints is assumed, then in a healthy manipulator the actual joint velocities $\dot{\mathbf{q}}_a$ equal the commanded velocities $\dot{\mathbf{q}}_c$. However, in the event of a locked-joint failure of the i-th joint, the corresponding element of $\dot{\mathbf{q}}_a$ is identically zero. Then, the actual end-effector velocity is given by

$$\dot{\mathbf{x}}_a = {}^iJ\dot{\mathbf{q}}_c, \tag{3}$$

This work was supported by Sandia National Labs under contract no. AL-3011 and by NSF under contract no. MIP-9708309.

0-7803-4465-0/98 $10.00 © 1998 IEEE

where ${}^iJ$ is the post-failure Jacobian, given by

$$ {}^iJ = [\ \mathbf{j}_1 \ \cdots \ \mathbf{j}_{i-1} \ \mathbf{0} \ \mathbf{j}_{i+1} \ \cdots \ \mathbf{j}_n\ ]. \quad (4) $$

It is assumed that the joint position sensors are still operational.

A common method for generating $\dot{\mathbf{q}}$ is the inverse kinematic scheme

$$ \dot{\mathbf{q}} = G\dot{\mathbf{x}}, \quad (5) $$

where G is a generalized inverse of J satisfying the Penrose condition $JGJ = J$. A frequently encountered generalized inverse is the pseudoinverse J^+, which yields the least squares minimum norm solution. For full rank J, the pseudoinverse can be expressed as $J^+ = J^T(JJ^T)^{-1}$.

In this work a general class of tasks characterized by sequences of point-to-point moves is considered. The commanded end-effector velocity is simply straight line motion towards the desired task position $\mathbf{x}_d$:

$$ \dot{\mathbf{x}}_c = K_e(\mathbf{x}_d - \mathbf{x}_a), \quad (6) $$

where $\mathbf{x}_a$ is the actual position of the end effector, and K_e is a constant position error gain that is adjusted when necessary to limit the commanded end-effector velocity to a maximum allowable value.

In the event of a locked-joint failure, the actual end-effector velocity in general will not be as commanded by (6). In particular, if joint i fails, the actual end-effector velocity is given by

$$ \dot{\mathbf{x}}_a = ({}^iJG)K_e(\mathbf{x}_d - \mathbf{x}_a). \quad (7) $$

Although $\dot{\mathbf{x}}_a$ may not drive the end effector directly towards the desired task position, it is of interest to know whether the end effector eventually converges (i.e., all its joints come to rest) to it.

III. Post-Failure Reachability

The workspace of a manipulator, in general, reduces after it experiences a failure [4, 12, 13]. However, under certain constraints, a task position can be guaranteed to be reachable by a redundant manipulator after an arbitrary joint failure along a trajectory. This is achieved by ensuring that the ranges of the joint values along the nominal trajectory never exceed the bounds of the joint values given by the self-motion manifold(s) of the desired task position [12].

The bounds of the self-motion manifolds can be directly computed by numerically tracing the manifold(s). Another more efficient way is to use the fact that at the extremum of a joint range, the self-motion manifold is tangent to the hyperplane defined by the extremum. Consequently, the contribution of that joint to the null motion of the manipulator is identically zero. It is easily shown that a joint i has a zero contribution to the null motion of the manipulator if and only if the Jacobian ${}^iJ = [\mathbf{j}_1 \cdots \mathbf{j}_{i-1}\ \mathbf{0}\ \mathbf{j}_{i+1} \cdots \mathbf{j}_n]$ is rank deficient [7] (this is referred to as a *semi-singularity* in [14]). If the condition for a joint to be at an extremum is not satisfied for any configuration corresponding to the desired end-effector position, then the range of that joint on the manifold is unconstrained, i.e., it spans the entire [0° 360°] range. The limiting values of the range of joint i are thus obtained by simultaneously solving the following equations:

$$ \mathbf{x}_d = f(\mathbf{q}), \quad \text{and} \quad (8) $$

$$ \mathbf{n}_{J_j}(i) = 0, \quad j = 1, \ldots, n-m, \quad (9) $$

where $\{\mathbf{n}_{J_1}, \ldots, \mathbf{n}_{J_{n-m}}\}$ represent any $n-m$ linearly independent null vectors of J. This idea is illustrated in Fig. 1.

The identified extrema partition the [0° 360°] ranges of the joints into a number of segments. The segments corresponding to the self-motion manifolds can then be identified by testing the midpoint of each of the obtained segments. Though this technique is a general one, its applicability depends upon the ease with which (8) and (9) can be solved.

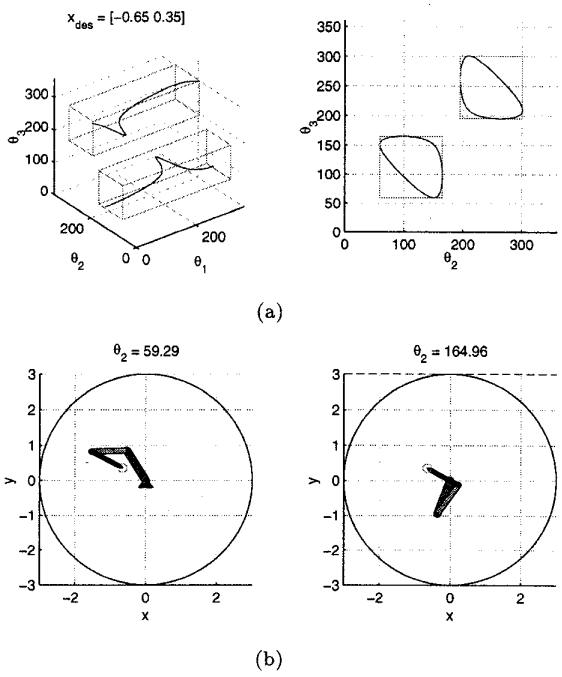

Fig. 1. (a) The self-motion curves and their bounding boxes for a 3-DOF unit link-length planar manipulator for an end-effector position $\mathbf{x}_{des} = [-0.65\ 0.35]^T$. (b) Configurations for which Joint 2 has extreme values over one of the two self-motion manifolds (${}^2J = [\mathbf{j}_1\ \mathbf{0}\ \mathbf{j}_3]$ rank deficient).

IV. Analysis of Convergence Behaviors

Although the reachability of a task position may be guaranteed after a failure along a trajectory, correct convergence to it may or may not be. It was shown in [11] that a manipulator may exhibit one of three behaviors after experiencing an undetected locked-joint failure: convergence to a "stationary" configuration, which may correspond to either the desired position (correct convergence), or to a position other than that desired (erroneous convergence), and no convergence.

A. Characterizing Erroneous Convergence

A manipulator gets "stuck" or converges to a configuration other than to one corresponding to the desired position, if and only if the failed joints alone are commanded nonzero velocities. This observation is formalized in the following theorem from [11].

Theorem 1: Consider a manipulator at a nonsingular configuration, driven by a generalized inverse control

$$\dot{\mathbf{q}}_c = G\dot{\mathbf{x}}_c, \tag{10}$$

where $G = W^{-1}J^T(JW^{-1}J^T)^{-1}$ for some symmetric $W > 0$. Let S be the set of the indices of the k locked joints, and let $\mathbf{j}_i$ and $\mathbf{w}_i$ denote the i-th columns of J and W respectively. Then:

1. Only the failed joints are commanded motion if and only if the commanded end-effector velocity vector $\dot{\mathbf{x}}_c$ lies in the space spanned by the columns corresponding to the failed joints of the Jacobian, i.e.,

$$\dot{\mathbf{q}}_c = \sum_{i\in S}\alpha_i\mathbf{e}_i \Longleftrightarrow \dot{\mathbf{x}}_c = \sum_{i\in S}\alpha_i\mathbf{j}_i, \tag{11}$$

for some $\alpha_i \in \mathbb{R}$, $i \in S$

2. Moreover, the failed joints are commanded nonzero velocities only if a post-failure weighted Jacobian is rank deficient, i.e.,

$$\dot{\mathbf{q}}_c = \sum_{i\in S}\alpha_i\mathbf{e}_i \neq \mathbf{0} \Longrightarrow {}^i(JW^{-1}) \text{ rank deficient}, \tag{12}$$

where ${}^i(JW^{-1}) \in \mathbb{R}^{m\times(n-k)}$ is obtained from JW^{-1} by zeroing the columns with indices $i \in S$.

□

The conditions of Theorem 1 can be used to determine configurations of erroneous convergence for a failed manipulator. For the sake of illustration, only single joint failures and identity weighting will be considered henceforth. Suppose the column of the Jacobian corresponding to a failed revolute joint i is expressed in standard Denavit-Hartenberg notation as

$$\mathbf{j}_i = \begin{bmatrix} \hat{\mathbf{z}}_{i-1} \times \mathbf{p}_i \\ \hat{\mathbf{z}}_{i-1} \end{bmatrix}, \tag{13}$$

where coordinate frame $(i-1)$ is attached to link $(i-1)$, the motion of joint i is along the $\hat{\mathbf{z}}_{i-1}$ axis, and $\mathbf{p}_i$ represents the position vector of the end effector expressed in the coordinate frame $(i-1)$. Then, if $\dot{\mathbf{x}}_v$ and $\dot{\mathbf{x}}_\omega$ represent the translational and rotational components of $\dot{\mathbf{x}}_c$, the first condition is equivalent to simultaneously satisfying the following conditions:

$$\dot{\mathbf{x}}_v^T\mathbf{p}_i = \dot{\mathbf{x}}_v^T\hat{\mathbf{z}}_{i-1} = 0, \quad \text{and} \tag{14}$$

$$\dot{\mathbf{x}}_\omega^T\hat{\mathbf{x}}_{i-1} = \dot{\mathbf{x}}_\omega^T\hat{\mathbf{y}}_{i-1} = 0. \tag{15}$$

With pseudoinverse control ($W = I$), the rank deficiency condition in Theorem 1, is equivalent to the i-th component of each of the $n-m$ linearly independent null vectors of J being identically zero [7]. Thus if $\{\mathbf{n}_{J_1}, \ldots, \mathbf{n}_{J_{n-m}}\}$ represent any $n-m$ linearly independent null vectors of J, then the second condition of Theorem 1 is equivalent to

$$\mathbf{n}_{J_j}(i) = 0, \quad j = 1, \ldots, n-m. \tag{16}$$

Equations (14)–(16) represent the conditions that must hold for erroneous convergence. For a given failure angle of a joint, these equations can be solved for the other joint variables to determine the problematic configurations.

B. Analyzing Stationary Configurations

After the stationary configurations of a manipulator are determined, an important question is whether a manipulator can be drawn into any of these configurations after a failure. The local behavior of the failed manipulator about a stationary point ($\mathbf{q}_0$) can be determined by analyzing the stability of the linearized system dynamics about the point. For $\dot{\mathbf{q}} = g(\mathbf{q})$, where $g(\mathbf{q}) = {}^iIGK_e(\mathbf{x}_d - \mathbf{x}_a)$, linearization about $\mathbf{q}_0$ yields:

$$\frac{d}{dt}\Delta\mathbf{q} = \left(\frac{\partial g}{\partial \mathbf{q}}|_{\mathbf{q}_0}\right)\Delta\mathbf{q} = \tilde{J}\Delta\mathbf{q}. \tag{17}$$

Since the components of the vectors $\Delta\mathbf{q}$, and $\frac{d}{dt}\Delta\mathbf{q}$ corresponding to the failed joint i are identically zero at all times after the failure, the matrix $\tilde{J}_i$, obtained from $\tilde{J}$ by removing the components corresponding to joint i, is examined for stability. While an antistable equilibrium point (where all eigenvalues of $\tilde{J}_i$ have positive real parts) poses no problem as far as erroneous convergence of the manipulator is concerned, a stable equilibrium point (all eigenvalues have negative real parts) acts as an attractor and is a potential problem. A stable

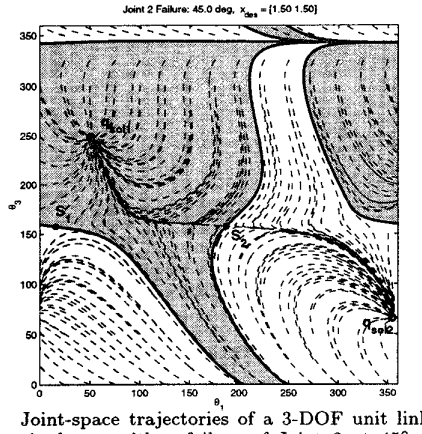

Fig. 2. Joint-space trajectories of a 3-DOF unit link length, planar manipulator, with a failure of Joint 2 at 45°. S_1 and S_2 represent the two stationary configurations, while $\mathbf{q}_{\mathbf{sol}_1}$ and $\mathbf{q}_{\mathbf{sol}_2}$ represent the two post-failure solutions corresponding to the desired position. The solid lines represent trajectories that are drawn to the stationary points; they also partition the joint space into the two basins. All trajectories (shown by dashed lines) that originate in the gray basin converge to $\mathbf{q}_{\mathbf{sol}_1}$, while those that originate in the unshaded basin converge to $\mathbf{q}_{\mathbf{sol}_2}$.

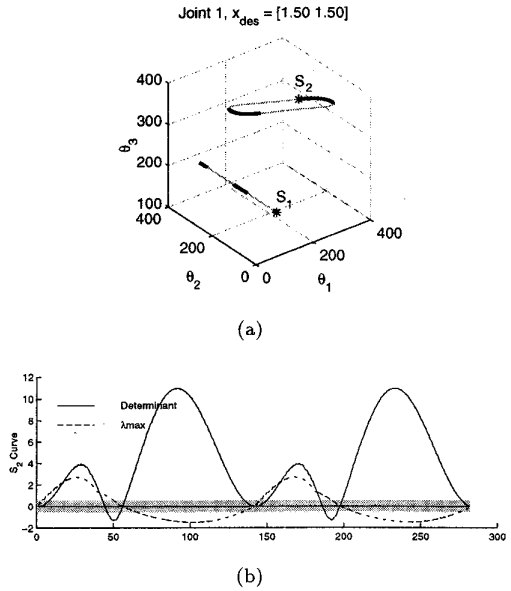

Fig. 3. Stationary curves for Joint 1 failures of a 3-DOF unit link length planar manipulator are shown in (a). S_1 and S_2 denote the two seed configurations used to trace these curves. The sink segments are shown with thin lines, while the non-sink segments are shown with thick lines. The segments are partitioned based on the behavior of the determinant and the real part of the eigenvalues of $\tilde{J}_1$ as shown, for S_2, in (b). The shaded area in (b) defines a "zero band" that is used to check for the zero crossings of the determinant curve.

stationary configuration is classified as a "sink". For an unstable equilibrium point (some eigenvalues have negative real parts), the stable modes can be used to trace the failure configurations for which the manipulator gets drawn to a stationary point. These traces, which are in general manifolds, also partition the workspace into distinct regions, or "basins". Since trajectories originating off the basin boundaries can never reach these boundaries, all trajectories are confined to the basins where they originate (see Fig. 2).

An important point to note is that unless the stationary points are sinks, the dimension of these boundary manifolds is at least two less than the dimension of the joint space (or the number of DOFs) of the manipulator. This is because the failure itself constrains one variable, reducing the dimension by one, while the additional reductions in dimension, if any, result due to the unstable modes. This implies that in the absence of sinks, the probability of a failure resulting in a manipulator configuration *on* a problematic manifold is zero.

C. Tracing and Classifying Stationary Manifolds

For an analysis of correct convergence, all potentially problematic stationary configurations in the manipulator's joint space must be identified. The loci of these stationary configurations (referred to as "stationary manifolds") must be generated for every possible joint failure. The first step in tracing a stationary manifold for a particular joint is to identify *one* stationary configuration for each distinct singularity of the failed arm. These stationary configurations represent the set of seed configurations that are grown to trace out the entire stationary manifold. Since (14)–(16) must hold at all stationary configurations, the loci of stationary configurations can be traced by simply starting at a seed that satisfies these conditions, and moving in a direction orthogonal to the gradients of the right hand side components of these equations. Doing this for each seed allows all the loci to be traced. In summary, a matrix M is formed by collecting the gradients, and joint motion in the null space of M traces the manifolds (see Fig. 3(a)). Methods such as those established for tracing self-motion manifolds [12] may be used to trace these stationary manifolds. The rank of M may drop along a trace, signifying the increase in the dimension of the null space, and hence a branching in the manifold. This is an issue that must be addressed in the implementation of this technique.

Sinks, being the real hindrance to correct convergence, must be identified on the stationary manifolds. Though this may be done by checking the eigenvalues of $\tilde{J}_i$ at each point on the discretized manifolds, a more efficient way is to evaluate the determinant of $\tilde{J}_i$, and check the eigenvalues only at the zero crossings of the determinant. This is because only at these zero crossings can the eigenvalues change sign. The stationary manifolds can thus be partitioned into "sink" and "non-sink" segments (see Fig. 3(b)).

V. Workspace Analysis

The post-failure convergence behavior of manipulators, in addition to being a function of other variables, is seen to be dependent on task placement. If failure detection is not available, or otherwise, not reliable, this knowledge can be exploited to better cope with failures. Through the characterization and classification of workspace regions, critical tasks can be placed in locations to which the manipulator can correctly converge even after an arbitrary joint failure.

Analyzing the workspace of a manipulator for failure tolerance involves checking for reachability and correct convergence. Based on the ideas presented in the foregoing sections, a systematic procedure can be developed to analyze a manipulator's workspace. For the given task model of point-to-point motion, a specified control scheme, and a desired task position, it is of interest to evaluate the entire workspace to determine the effect of the initial task position on the convergence behavior of a manipulator when anticipating undetected locked-joint failures. Some concerns when evaluating a candidate initial task position are: For what percentage of the trajectories originating on the self-motion manifolds of the initial position can reachability of the desired position be guaranteed? If reachability cannot be guaranteed for a failure along the entire trajectory, then for what percentage of the trajectory can reachability be guaranteed? How much does the percentage reachability change with the initial configuration? That is, how sensitive is reachability to a choice of the initial configuration? Similarly, questions about correct convergence to the desired position can be posed for trajectory portions guaranteeing reachability.

For a given desired task position, the following procedure allows the workspace to be evaluated for identifying the suitability of different initial positions for the task. (An analogous procedure can be performed when an initial position is specified instead.) The first step of the procedure is to discretize the entire workspace. The discretized positions in the workspace represent the set of initial positions to be evaluated. Since, in general, a redundant manipulator can reach each of these positions with an infinite number of configurations, a set of initial configurations must be considered. This set of configurations is obtained from the discretized self-motion manifold(s) corresponding to the initial configuration. The procedure for the analysis is summarized in the following pseudocode.

- Generate $\mathcal{B}_{\mathbf{d}}$
  (the union of the bounding boxes of all the self-motion manifolds of $\mathbf{x}_{\mathbf{d}}$, the desired task position)
- Discretize the workspace to get a set of initial positions $\mathbf{x}_{\mathbf{i}}(i)$, $i = 1 : n_{\mathbf{x}_{\mathbf{i}}}$

for $i = 1 : n_{\text{jts}}$ (for each joint)
- Generate $\mathcal{S}_i$ (the union of all the stationary manifolds) and classify $\mathcal{S}_i$ into sinks/non-sinks

end

for $i = 1 : n_{\mathbf{x}_{\mathbf{i}}}$ (for each initial end-effector position)
- Generate the self-motion manifold(s) for $\mathbf{x}_{\mathbf{i}}(i)$

for $j = 1 : n_{\mathbf{q}_{\mathbf{i}}}$ (for each discretized configuration on the manifold(s))
- Compute the forward trajectory $\mathcal{T}_j$ to $\mathbf{x}_{\mathbf{d}}$ for the healthy manipulator
- Compute $\mathcal{T}_{j_{\mathbf{in}}}$, the portion of $\mathcal{T}_j$ inside $\mathcal{B}_{\mathbf{x}_{\mathbf{d}}}$

for $\mathcal{T}_{j_{\mathbf{in}}}$

for $i = 1 : n_{\text{jts}}$ (for each joint)
- Compute the intersection of the range of motion of joint i over $\mathcal{T}_{j_{\mathbf{in}}}$, with the corresponding range over sink($\mathcal{S}_i$)

for $\mathcal{T}_{j_{\mathbf{in}}} \cap \mathcal{S}_i$
- For each discretized point on the overlap, assume a failure of joint i and check whether or not the manipulator converges to $\mathbf{x}_{\mathbf{d}}$

end

($\mathcal{T}_{j_{\mathbf{in}}} \cap \mathcal{S}_i$ empty $\Rightarrow$ The task is tolerant to joint i failures over $\mathcal{T}_{j_{\mathbf{in}}}$)

end

($\mathcal{T}_{j_{\mathbf{in}}} \cap \mathcal{S}_i$ empty for $i = 1 : n_{\text{jts}} \Rightarrow$ The task is tolerant to an arbitrary joint failure over $\mathcal{T}_{j_{\mathbf{in}}}$)

end

end

end

The data obtained from the implementation of this procedure can be interpreted in a variety of ways; however, the questions posed earlier in this section are best addressed by the following measures:

$\mathcal{R}_{100}$: The percentage of configurations considered for $\mathbf{x}_{\mathbf{i}}$, for which reachability of $\mathbf{x}_{\mathbf{d}}$ can be guaranteed for the failure of a joint along the entire length of the nominal trajectory.

$\mathcal{R}_{\text{avg}}$: The percentage length of the nominal trajectory for which reachability to $\mathbf{x}_{\mathbf{d}}$ can be guaranteed for the failure of a joint, averaged over all considered configurations.

$\mathcal{R}_{\text{sens}}$: The difference between the maximum and minimum, over all considered configurations, of the percentage of the trajectory for which reachability to $\mathbf{x}_{\mathbf{d}}$ can be guaranteed for a joint failure. This measure reflects the sensitivity of reachability to a choice of the initial configuration corresponding to $\mathbf{x}_{\mathbf{i}}$.

Analogous measures for complete fault tolerance (correct convergence), over trajectory segments guaranteeing reachability, are given by $\mathcal{F}_{100}$, $\mathcal{F}_{\text{avg}}$, and $\mathcal{F}_{\text{sens}}$ respectively. All measures are computed for the possibility of a failure of a specific (known) joint, as well as that of an arbitrary (unknown) joint.

An Illustration

The application of the workspace analysis procedure proposed above is illustrated for the example of a 3-DOF planar manipulator with unit link lengths. The desired position considered in this example of a point-to-point motion task is $\mathbf{x}_{\mathbf{d}} = [1.5\ 1.5]^T$. The workspace

of the manipulator is sampled on an equally spaced square grid, using 2032 samples. Each of these samples is evaluated as a candidate initial position for the task. The stationary manifolds for this example are generated and partitioned into sink and non-sink segments as discussed in Section IV-C. The bounding box $\mathcal{B}_{\mathbf{x}_d}$ for the single self-motion manifold corresponding to $\mathbf{x}_d$ is computed using the technique outlined in Section III. The bounds are: [−24.30° 114.30°], [−111.80° 111.80°], and [−111.80° 111.80°], for Joints 1, 2, and 3 respectively. In Fig. 4 the workspace is shaded as a function of four of the six proposed measures: $\mathcal{R}_{100}$, $\mathcal{R}_{\text{avg}}$, $\mathcal{R}_{\text{sens}}$, and $\mathcal{F}_{100}$, considering arbitrary failures. These plots demonstrate how the failure tolerance properties of the manipulator change over the workspace. Since the measures change in a continuous manner over the workspace, these plots can be used to identify regions that guarantee a certain level of failure tolerance. It is noted that in general all regions with nonzero reachability measures $\mathcal{R}_{100}$ and $\mathcal{R}_{\text{avg}}$ exhibit high values of the corresponding comprehensive fault tolerance measures $\mathcal{F}_{100}$ and $\mathcal{F}_{\text{avg}}$ (not shown). In other words, most trajectory segments that guarantee the reachability of the task position also guarantee correct convergence. Though this is true for $\mathbf{x}_d$ in this example, it may not be guaranteed for an arbitrary choice of task position. It was also seen that the comprehensive sensitivity measure $\mathcal{F}_{\text{sens}}$ (not shown) is very low over the workspace, implying that if reachability is guaranteed, correct convergence has little dependence on the initial configuration of the manipulator.

VI. Conclusion

In this work a general procedure for evaluating the failure tolerance properties of manipulators performing point-to-point motion tasks was presented. This procedure allows regions of the workspace to be classified based on their influence on the failure tolerance properties of a manipulator with respect to a task. Since no closed form expressions to guarantee correct convergence exist, brute force evaluations to check for the effect of certain failures become necessary over some portions of the workspace. However, the procedure based on the developed analysis tools allows for an intelligent evaluation of the workspace, thereby minimizing the number of brute force checks. Using workspace information for task placement is an effective approach to coping with failures, with or without failure detection.

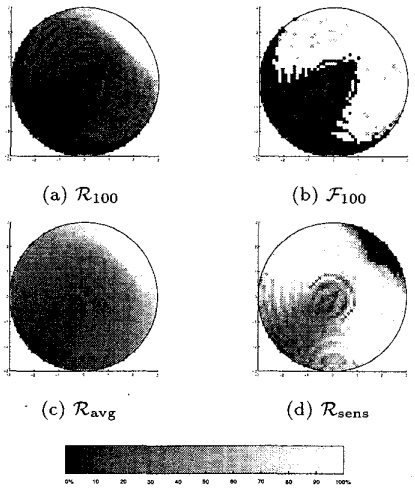

Fig. 4. Workspace shaded as a function of $\mathcal{R}_{100}$, $\mathcal{F}_{100}$, $\mathcal{R}_{\text{avg}}$, and $\mathcal{R}_{\text{sens}}$, for arbitrary joint failures ($\mathbf{x}_d = [1.5\ 1.5]^T$).

References

[1] B. S. Dhillon, *Robot Reliability and Safety*, Springer-Verlag, New York, 1991.

[2] R. Colbaugh and M. Jamshidi, "Robot manipulator control for hazardous waste-handling applications," *J. Robot. Syst.*, vol. 9, no. 2, pp. 215–250, 1992.

[3] E. C. Wu, J. C. Hwang, and J. T. Chladek, "Fault-tolerant joint development for the space shuttle remote manipulator system: Analysis and experiment," *IEEE Trans. Robot. Automat.*, vol. 9, no. 5, pp. 675–684, Oct. 1993.

[4] A. K. Pradeep, P. J. Yoder, R. Mukundan, and R. J. Schilling, "Crippled motion in robots," *IEEE Trans. Aerospace Elect. Syst.*, vol. 24, no. 1, pp. 2–13, Jan. 1988.

[5] C. L. Lewis and A. A. Maciejewski, "Dexterity optimization of kinematically redundant manipulators in the presence of failures," *Comput. Elect. Eng.*, vol. 20, no. 3, pp. 273–288, May 1994.

[6] C. J. J. Paredis, W. K. F. Au, and P. K. Khosla, "Kinematic design of fault tolerant manipulators," *Comput. Elect. Eng.*, vol. 20, no. 3, pp. 211–220, May 1994.

[7] R. G. Roberts and A. A. Maciejewski, "A local measure of fault tolerance for kinematically redundant manipulators," *IEEE Trans. Robot. Automat.*, vol. 12, no. 4, pp. 543–553, Aug. 1996.

[8] M. L. Visinsky, J. R. Cavallaro, and I. D. Walker, "A dynamic fault tolerance framework for remote robots," *IEEE Trans. Robot. Automat.*, vol. 11, no. 4, pp. 477–490, Aug. 1995.

[9] Y. Ting, S. Tosunoglu, and D. Tesar, "A control structure for fault-tolerant operation of robotic manipulators," *Proc. 1993 Int. Conf. Robot. Automat.*, pp. 684–690, (Atlanta, Georgia), May 2-6 1993.

[10] M. L. Visinsky, J. R. Cavallaro, and I. D. Walker, "Robotic fault detection and fault tolerance: A survey," *Reliab. Eng. Syst. Safety*, vol. 46, pp. 139–158, 1994.

[11] M. Goel, A. A. Maciejewski, and V. Balakrishnan, "An analysis of the post-fault behavior of robotic manipulators," *Proc. 1997 Int. Conf. Robot. Automat.*, pp. 2583–2588, (Albuquerque, NM), Apr. 20-25 1997.

[12] C. L. Lewis and A. A. Maciejewski, "Fault tolerant operation of kinematically redundant manipulators for locked joint failures," *IEEE Trans. Robot. Automat.*, vol. 13, no. 4, pp. 622–629, Aug. 1997.

[13] C. J. J. Paredis and P. K. Khosla, "Mapping tasks into fault tolerant manipulators," *Proc. 1994 Int. Conf. Robot. Automat.*, pp. 696–703, (San Diego, CA), May 8-13 1994.

[14] C. L. Lück and S. Lee, "Self-motion topology for redundant manipulators with joint limits," *Proc. 1993 Int. Conf. Robot. Automat.*, pp. 626–631, (Atlanta, Georgia), May 2-6 1993.